THE JOURNAL OF PHYSICAL CHEMISTRY B

Article

pubs.acs.org/JPCB

Differences in Proton-Coupled Electron-Transfer Reactions of Flavin Mononucleotide (FMN) and Flavin Adenine Dinucleotide (FAD) between Buffered and Unbuffered Aqueous Solutions

Serena L. J. Tan, Jia Min Kan, and Richard D. Webster*

Division of Chemistry and Biological Chemistry, School of Physical and Mathematical Sciences, Nanyang Technological University, Singapore 637371

Supporting Information

ABSTRACT: The electrochemical reduction mechanisms of flavin mononucleotide (FMN) in buffered aqueous solutions at pH 3−11 and unbuffered aqueous solutions at pH 2−11 were examined in detail using variable-scan-rate cyclic voltammetry (ν = 0.1−20 V s^{-1}), controlled-potential bulk electrolysis, UV−vis spectroscopy, and rotating-disk-electrode voltammetry. In buffered solutions at pH 3−5, FMN undergoes a two-electron/two-proton ($2e^-/2H^+$) reduction to form $FMNH_2$ at all scan rates. When the buffered pH is increased to 7−9, FMN undergoes a $2e^-$ reduction to form FMN^{2-}, which initially undergoes hydrogen bonding with water molecules, followed by protonation to form $FMNH^-$. At a low voltammetric scan rate of 0.1 V s^{-1}, the protonation reaction has sufficient time to take place. However, at a higher scan rate of 20 V s^{-1}, the proton-transfer reaction is outrun, and upon reversal of the scan direction, less of the $FMNH^-$ is available for oxidation, causing its oxidation peak to decrease in magnitude. In unbuffered aqueous solutions, three major voltammetric waves were observed in different pH ranges. At low pH in unbuffered solutions, where $[H^+] \geq [FMN]$, $(FMN)H^-$ undergoes a $2e^-/2H^+$ reduction to form $(FMNH_2)H^-$ (wave 1), similar to the mechanism in buffered aqueous solutions at low pH. At midrange pH values (unbuffered), where pH ≤ pK_a of the phosphate group and $[FMN] \geq [H^+]$, $(FMN)H^-$ undergoes a $2e^-$ reduction to form $(FMN^{2-})H^-$ (wave 2), similar to the mechanism in buffered aqueous solutions at high pH. At high pH (unbuffered), where pH ≥ pK_a = 6.2 of the phosphate group, the phosphate group loses its second proton to be fully deprotonated, forming $(FMN)^{2-}$, and this species undergoes a $2e^-$ reduction to form $(FMN^{2-})^{2-}$ (wave 3).

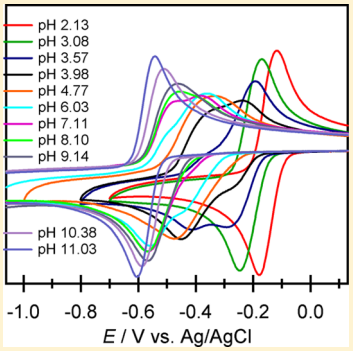

1. INTRODUCTION

Flavin cofactors such as flavin adenine dinucleotide (FAD) and flavin mononucleotide (FMN) (see Scheme 1) are the electroactive components of flavoenzymes, which catalyze many redox reactions in biological systems, because of their ability to act as intermediaries by accepting electrons from many functional groups and donating the electrons to other molecules.[1−5] Although the cofactors of the flavoenzymes are the same, different classes of flavoenzymes catalyze vastly different electron-transfer reactions.[6] For example, some catalyze two-electron transfers between an electron donor and acceptor,[6] flavodoxins catalyze one-electron transfers between an electron donor and acceptor,[6,7] and another catalyzes electron-transfer reactions between a two-electron donor and a one-electron acceptor.[8,9]

The difference between the different classes of flavoenzymes is reported to be due to different intermolecular interactions with the flavoenzymes and the water molecules that are either buried within the protein structure or present in the bulk solution. For example, the electroactive site of the flavin cofactor in NADH-cytochrome b_5 reductase (where NADH is the reduced form of nicotinamide adenine dinucleotide, NAD^+) is situated in a large crevice between the two domains of the flavoenzyme[10] and is accessible to water molecules in the solution. Thus, it is able to undergo a two-electron/two-proton ($2e^-/2H^+$) reduction to $FADH_2$ when NAD^+ is not bound.[8] When NAD^+ is bound, changes in intermolecular interactions causes it to be able to stabilize the flavosemiquinone form, enabling it to donate one electron to one-electron acceptors.

We recently reported the proton-coupled electron-transfer (PCET) mechanism of riboflavin in the aprotic organic solvent dimethyl sulfoxide (DMSO).[11] However, the PCET reactions that occur in DMSO might not be the same as for flavoenzymes for which the flavin cofactor is accessible by water molecules in solution. Many electrochemical studies have been conducted on flavins in buffered aqueous solutions, and it is now widely accepted that, in aqueous media, the fully oxidized flavin (FMN) is reduced to flavohydroquinone ($FMNH_2$) in "one step" in a $2e^-/2H^+$ reduction (by one step, it is meant that the individual electron-transfer and proton-transfer steps occur in one observable voltammetric process).[12−21] However, it is unlikely that the protonation will occur at very high pH in unbuffered solutions, as there will be insufficient protons in solution to be transferred in this reduction process.

Received: July 15, 2013
Revised: September 24, 2013
Published: September 30, 2013

dx.doi.org/10.1021/jp4069619 | J. Phys. Chem. B 2013, 117, 13755−13766

Scheme 1. Structures of Riboflavin (Vitamin B_2), Flavin Mononucleotide, and Flavin Adenine Dinucleotide

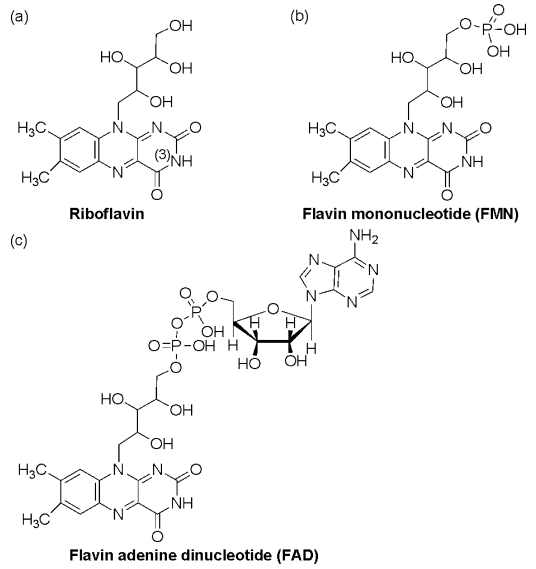

Quinones (Q), whose electrochemical properties are similar to flavins, undergo two one-electron reduction processes in aprotic organic solvents to form first the semiquinone anion radicals ($Q^{\bullet -}$) and then the dianions (Q^{2-}). Recent studies have shown that, when a significant amount of water is added to an organic solution containing quinones, the two reduction peaks merge such that the quinone is directly reduced to the hydrogen-bonded dianion $[Q^{2-}(H_2O)_x]$ in one two-electron process.[22] In a related study of quinones in unbuffered aqueous solutions,[23] it was argued that, when the proton concentration is lower than the quinone concentration, the quinone undergoes a $2e^-$ reduction to the strongly hydrogen-bonded dianion Q^{2-}, which exists in water as a mixture of Q^{2-}, QH^-, and QH_2 because of the basicity of the dianion. It is proposed that this mechanism could be extended to flavins in both unbuffered aqueous solutions and aqueous solutions buffered at very high pH, in which the proton concentrations are similarly lower than the flavoquinone concentration.

To better understand the electron-transfer mechanism in flavoenzymes in which the flavin cofactor is accessible to water molecules, this study investigated the importance of hydrogen bonding in buffered and unbuffered aqueous solutions, the pH dependence of the reaction mechanisms, and the likely mechanisms at different pH values. All voltammetric experiments were conducted under an argon atmosphere to avoid complications of reduced flavins reacting with dissolved molecular oxygen. The electrochemical data obtained in unbuffered solutions were carefully modeled using digital simulation techniques to explain the appearance of all detected voltammetric peaks.

2. EXPERIMENTAL SECTION

2.1. Chemicals. Flavin mononucleotide (FMN) and flavin adenine dinucleotide (FAD) were obtained from Alfa Aesar and were of analytical reagent grade. Potassium chloride (KCl) was obtained from Goodrich Chemical Enterprise. Acetic acid, phosphoric acid, and boric acid used in Britton–Robinson buffers were obtained from Sinopharm Chemical Reagent Co., Ltd, and were of analytical reagent grade.

2.2. Electrochemical Procedures. Cyclic voltammetry (CV) experiments were conducted with a computer-controlled Eco Chemie Autolab PGSTAT 100 instrument with an ADC fast scan generator. The working electrode was a 1-mm-diameter planar glassy carbon (GC) disk that was polished frequently with 1-μm alumina powder and used in conjunction with a Pt-wire auxiliary electrode and a Ag/AgCl reference electrode. Unbuffered solutions were prepared by making a solution of FMN or FAD in 0.4 M KCl in deionized water and adjusting the pH using carefully diluted solutions of HCl and NaOH. Buffered solutions were prepared by adding equal volumes of acetic acid, phosphoric acid, and boric acid (0.04 mol L^{-1}) and then adjusting the pH to the desired value using a NaOH solution (0.2 mol L^{-1}). This solution was then added to FMN to form a 1 mM FMN solution in Britton–Robinson buffer. Solutions of FMN (1 mM FMN in Britton–Robinson buffer and 1–5 mM FMN and 0.4 M KCl in deionized water) for voltammetric analysis were deoxygenated by purging with high-purity argon gas, and all voltammetric experiments were conducted at 22 (±2) °C in a Faraday cage. Digital simulations of the CV data were performed using the DigiElch 6 software package purchased from Gamry Instruments.

Controlled potential electrolysis was performed in a two-compartment electrolysis cell using a GC rod as the working electrode, Pt mesh as the auxiliary electrode, and a Ag/AgCl (3 M KCl) reference electrode.

2.3. Spectroscopic Experiments. UV–vis spectra were obtained using a thin-layer quartz cell at 22 (±2) °C and recorded on a Perkin-Elmer model Lambda 750 UV–vis–NIR spectrophotometer.

3. RESULTS AND DISCUSSION

3.1. FMN (1 mM) in Buffered Aqueous Solutions. *3.1.1. Cyclic Voltammetry.* Cyclic voltammetric scans were run at variable scan rates of 0.1–20 V s^{-1} in buffered solutions with pH values of 3, 5, 7, 9, and 11 (Figure 1). At pH 3–5, the initial

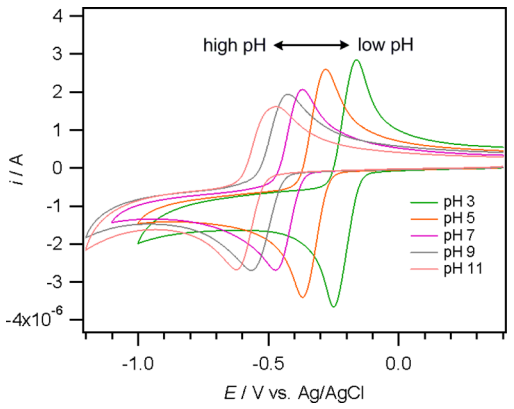

Figure 1. Cyclic voltammograms of 1 mM FMN in solutions buffered at pH 3–11 at 0.1 V s^{-1} using a 1-mm-diameter planar GC electrode.

species in solution is likely to be FMN, as the pK_a of FMN is approximately 10,[13,14,16,19,27–33] so FMN will not lose its amine proton in low-pH solutions. In this pH range, the acid concentration is sufficient to donate one or two protons to the analyte, and it is likely that FMN undergoes a two-electron/two-proton reduction to form the fully reduced flavin $FMNH_2$. This is further substantiated by the shift of 60 mV per pH unit in this pH range, indicating that the numbers of electrons and

dx.doi.org/10.1021/jp4069619 | J. Phys. Chem. B 2013, 117, 13755–13766

protons transferred during the reduction are equal. Controlled potential electrolysis with coulometry confirmed that two electrons were transferred per molecule, indicating that two protons were also transferred during this reduction wave.

At pH 7–9, the initial species is still FMN, but because the proton concentration is much lower than the analyte concentration, the reduced forms of FMN might not immediately undergo a protonation reaction. In a previous study concerning the reduction of quinones in organic solvents with varying water contents, when the water level was very high, hydrogen-bonding interactions caused the two reduction peaks to merge so that the quinones were reduced directly to Q^{2-} in one step.[22] Thus, it is postulated that, in this aqueous environment of neutral to moderately basic pH, FMN is electrochemically reduced by two electrons to FMN^{2-} and then initially undergo a series of hydrogen-bonding reactions with water. Because of its basicity, FMN^{2-} is then able to extract a proton from the buffer molecules to form $FMNH^-$.[23] It was observed that the shift per pH unit in this range decreased significantly from 60 mV. However, a shift of 30 mV per pH unit was not expected because a mixture of different species are likely to be formed, which can be detected as distinct oxidation peaks in the cyclic voltammograms at higher scan rates. $FMNH^-$ and the hydrogen-bonded FMN^{2-} can undergo oxidation at different potentials, giving rise to two oxidative peaks during the reverse scan (I_{ox} and II_{ox} in Figure 2). The actual ratio of the species present depends on the equilibrium and rate constants of the protonation and hydrogen-bonding reactions. The two overlapping oxidative peaks are observed only at high scan rates at pH 9, although it is likely that two oxidative peaks were also present at lower scan rates. An explanation for the visible separation of the peaks at higher scan rates could be a relatively slow equilibrium between the hydrogen-bonded dianion and $FMNH^-$, so that both species are voltammetrically detectable only at higher scan rates.

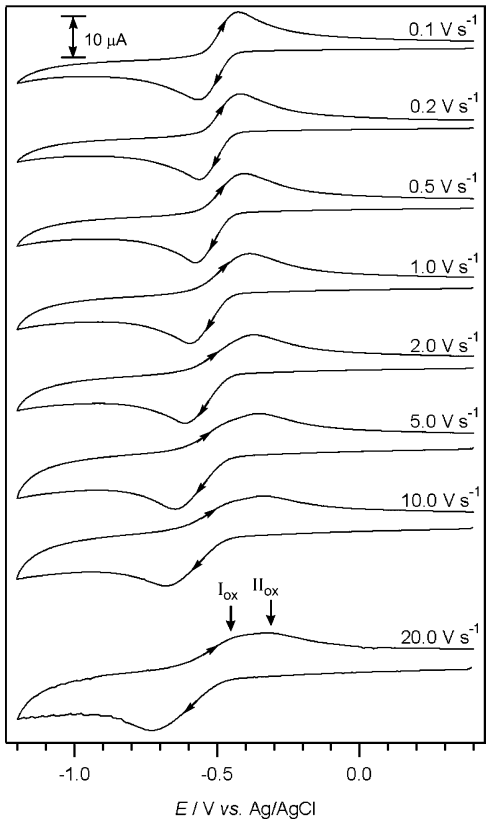

Figure 2. Variable-scan-rate cyclic voltammograms of 1 mM FMN in a solution buffered at pH 9 using a 1-mm-diameter planar GC electrode. Data were scaled by multiplication by $\nu^{-0.5}$.

At pH 11, the pH > pK_a(FMN), thus the initial species present is FMN^- (FMN with the N(3) deprotonated). After a two-electron reduction and various hydrogen-bonding and protonation reactions, a mixture of hydrogen-bonded FMN^{2-} and $FMNH^-$ is formed. Similarly to those observed at pH 9, the cyclic voltammograms obtained at pH 11 show two separate oxidation peaks at higher scan rates, whereas at lower scan rates, the oxidation peak is especially broad, indicating the possibility that it could comprise two oxidation peaks (see Figure S4 in the Supporting Information).

It is postulated that, for higher pH values (pH 9–11) and low scan rates, the major reduced species present is $FMNH^-$. As the scan rates increases, the protonation reaction of hydrogen-bonded FMN^{2-} is outrun; hence, more of the hydrogen-bonded FMN^{2-} species (oxidized during I_{ox}) and less of $FMNH^-$ (oxidized during II_{ox}) are present near the electrode surface during the oxidative scan. Indeed, for the cyclic voltammograms recorded at scan rates between 5 and 20 V s^{-1}, it can be observed that the first oxidation peak (I_{ox}) increases in size relative to the second oxidation peak (II_{ox}), which decreases in size as the scan rate increases.

3.1.2. Controlled Potential Electrolysis. To determine the main species present before and after reduction at each pH, a series of bulk electrolysis and UV–vis experiments were conducted. Controlled potential bulk electrolysis was run for 2 mM solutions of FMN in solutions buffered at pH 3, 5, 7, 9, and 11. At each pH, coulometry measurements indicated that two electrons were transferred per molecule over the long electrolysis time scale.

At acidic pH, the color changed from fluorescent yellow (FMN) to a greenish-brown and finally to an orangish-brown after two electrons had been transferred per FMN molecule. However, at basic pH, the color change was not as obvious, gradually changing from a fluorescent yellow to a dull yellow after two electrons had been transferred per FMN molecule. It was previously reported that $FMNH^-$ is a dull yellow color, whereas the anionic radical $FMN^{\bullet -}$ is red and the neutral radical $FMNH^{\bullet}$ is blue.[24]

Cyclic voltammograms were recorded with a 1-mm-diameter planar GC electrode before bulk electrolysis, after one electron had been transferred per molecule, and finally after two electrons had been transferred per molecule. For each pH, it was observed that, after one electron had been transferred, the initial current reading at +0.4 V (vs Ag/AgCl) in the cyclic voltammograms shifted upward to positive currents, indicative of the presence of a closely related species existing in a reduced state. After the transfer of two electrons per molecule, the current (measured at +0.4 V) shifted farther upward, indicating that more of the reduced species had been formed. However, because the CV scans commenced from a potential that was positive enough to oxidize the charged species back to the starting material (fully oxidized FMN), the cyclic voltammograms obtained still appeared to be identical to that of the fully oxidized FMN (starting material), the only difference being the position of zero current. Therefore, under acidic conditions of pH 3–5, FMN goes through a chemically reversible $2e^-/2H^+$ reduction to form $FMNH_2$ (Figure 3a).

dx.doi.org/10.1021/jp4069619 | J. Phys. Chem. B 2013, 117, 13755–13766

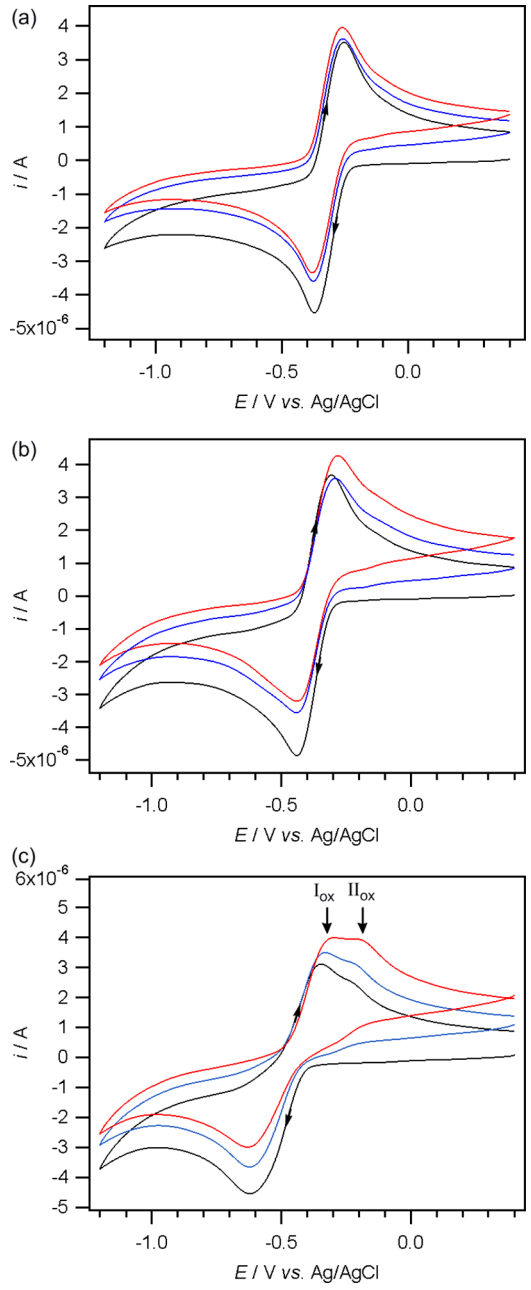

Figure 3. Cyclic voltammograms of 2 mM FMN at 0.1 V s^{-1} using a 1-mm-diameter planar GC electrode, before electrolysis (black line), after transfer of one electron per molecule (blue line), and after transfer of two electrons per molecule (red line) in aqueous solutions buffered at pH (a) 5, (b) 7, and (c) 9.

However, for pH 7–9, the cyclic voltammograms recorded after electrolysis showed the appearance of two closely spaced reduction and oxidation peaks (I_{ox} and II_{ox}) (Figure 3b,c). In this pH range, the concentration of free protons is much lower than the concentration of flavins, and thus, the compound does not follow the same reduction pathway as in acidic solutions. We postulate that the observation of two more closely spaced reduction and oxidation peaks (or shoulders in the forward and reverse voltammetric waves at pH 9) is due to the basicity of FMN^{2-} and its ability to deprotonate the buffer and the fact that the time scale of the electrolysis experiment is long (>1 h), so that the proton-transfer reaction has time to take place and reach equilibrium.[23] This will give rise to an equilibrium of FMN^{2-}, $FMNH^{-}$, and $FMNH_2$, with the major species present depending on the pH of the solution and the pK_a of each of the species.[23] When a cyclic voltammogram is run after the two-electron electrolysis at pH 9, a very broad reduction process with a shoulder is detected, and when the scan direction is reversed, two clear oxidation peaks are detected, because of the number of reduced species existing in the bulk solution (Figure 3c).

The observation of FMN^{2-}, $FMNH^{-}$, and $FMNH_2$ in the bulk solution after electrolysis is further substantiated by the UV–vis spectra of the two-electron-reduced species obtained at each pH.

3.1.3. UV–Vis Experiments. UV–vis spectra were collected before electrolysis and again after two electrons had been transferred per flavin molecule, to determine whether any structural changes occurred within the chromophore and to identify the species present in the bulk solution.

As shown in Figure 4, the UV–vis spectra of FMN at pH 3–9 were identical, with peaks at 446, 370, and 265 nm, but the

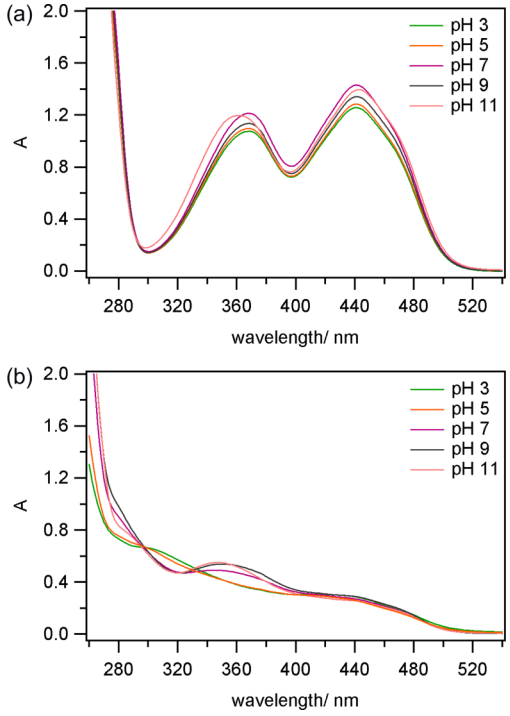

Figure 4. UV–vis spectra of 2 mM FMN in aqueous solutions buffered at pH 3–11 (a) before bulk electrolysis and (b) after transfer of two electrons per molecule of FMN during bulk electrolysis.

spectrum of FMN at pH 11 was slightly shifted, with peaks at 444, 355, and 265 nm. This indicates that, at pH 11, FMN likely exists in the deprotonated form, as the pK_a of FMN is close to 10.[13,14,16,19,24–33]

After two electrons had been transferred per molecule, significant differences among the two-electron-reduced compounds at the various pH values could be observed. For pH 3 and 5, two shoulder absorbances with maxima around 400 and 280 nm and a large peak at 245 nm were observed. However, for pH 9 and 11, a small peak with a maximum at 350 nm, a large peak at 255 nm, and a shoulder around 290 nm were observed. This indicates that, after two electrons had been transferred, the products of reduction under acidic and basic conditions had slightly different structures. UV–vis data of the

dx.doi.org/10.1021/jp4069619 | J. Phys. Chem. B 2013, 117, 13755–13766

different flavin species obtained by chemical methods, collected by Hemmerich et al.[25] and Dudley et al.,[26] further substantiate the hypothesis that, at pH 3−9, the initial species is FMN whereas, at pH 11, the initial species is likely to be FMN^-.[24−26]

The UV−vis spectrum of the species after electrolysis at pH 3−5 is closely similar to that obtained by Hemmerich et al.[25] and Dudley et al.[26] for $FMNH_2$, as well as that obtained by Malinowski et al.[34] for $FADH_2$, which has an identical chromophore. The UV−vis spectrum of the species after electrolysis at pH 7−11 resembles the UV−vis spectrum reported for $FMNH^-$.[24] This not only substantiates the conclusion that the final products at pH 3−5 and 7−11 are $FMNH_2$ and $FMNH^-$, respectively, but helps to narrow the range for the pK_a of $FMNH_2$ to be between 5 and 7. Indeed, data collected by Hemmerich et al. indicated that the pK_a of $FMNH_2$ is around 6.2.[25]

3.1.4. Electron-Transfer Mechanism of FMN in Buffered Aqueous Solutions. A reduction mechanism for FMN in buffered aqueous solutions can be proposed based on the voltammetric and spectroscopic experiments. For acidic aqueous environments with pH 3−5, FMN undergoes a $2e^-/2H^+$ reduction directly to $FMNH_2$ at all scan rates (Scheme 2).

Scheme 2. Voltammetrically Induced Proton-Coupled Electron-Transfer Reduction Mechanism of FMN in Aqueous Solutions Buffered at pH 3−5, Studied by Cyclic Voltammetry over a Range of Scan Rates and Concentrations

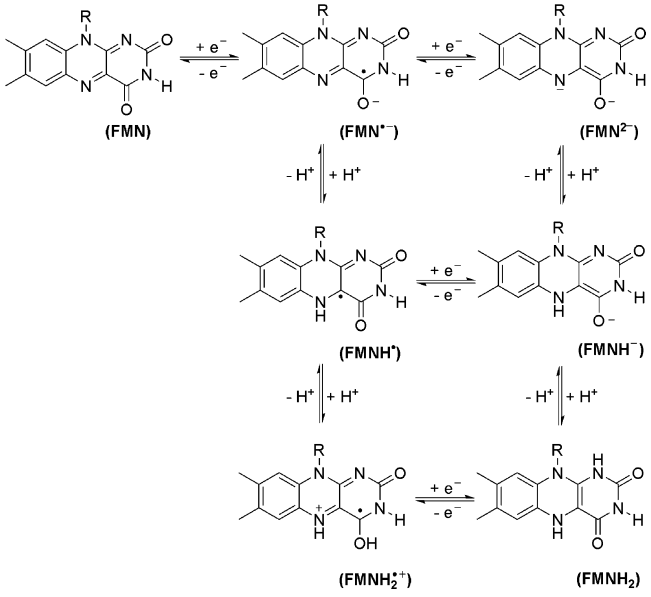

A UV−vis spectrum of the two-electron-reduced species after electrolysis confirmed that the major species present in solution is $FMNH_2$, as it agrees with previous UV−vis studies of the flavin compounds.[24] The intense colors observed during the bulk reduction suggest that some of the intermediate radical compounds might have a finite lifetime (possibly due to homogeneous reactions between the highly reduced $FMNH_2$ and the starting material) before all are ultimately converted to $FMNH_2$ as the electrolysis progresses.

For basic aqueous environments at pH 7−9 (Scheme 3), the pH is lower than the pK_a of FMN; thus, the species in solution before reduction is still the neutral fully oxidized flavin FMN. Bulk electrolysis confirmed that two electrons are transferred

Scheme 3. Voltammetrically Induced Proton-Coupled Electron-Transfer Reduction Mechanism of FMN in Aqueous Solutions Buffered at pH 7−11, Studied by Cyclic Voltammetry over a Range of Scan Rates and Concentrations

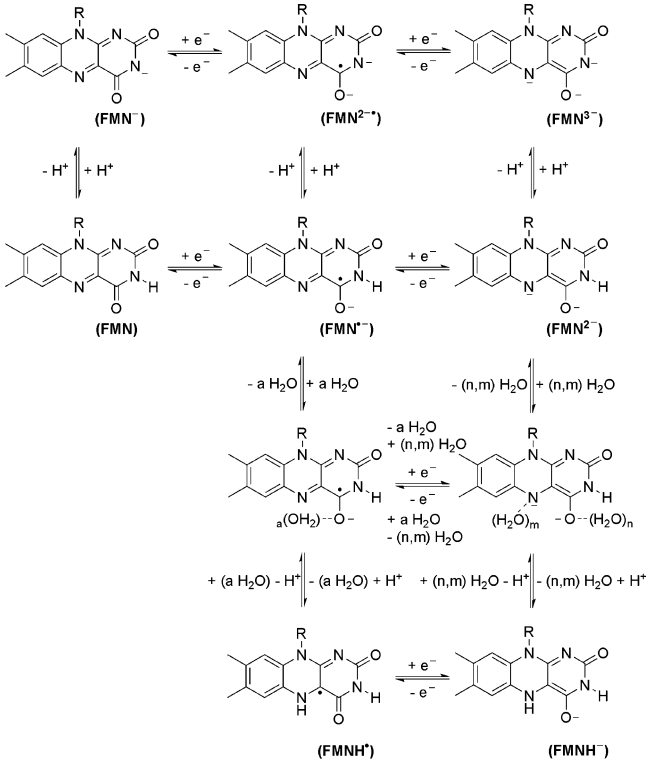

per molecule of FMN, and the lack of significant color changes suggests that FMN is reduced by two electrons to the dianion FMN^{2-}. During electrolysis, the time scale is long enough for the dianion to extract a proton from the buffer molecules, forming $FMNH^-$.

Nevertheless, the time scale of the experiment is shorter for cyclic voltammetry. Thus, for low scan rates at pH 7−9, there is sufficient time for the proton-transfer reaction to take place after the dianion is formed. As the scan rate increases, the reverse oxidation wave is split into two processes, possibly because of the presence of the hydrogen-bonded dianion (FMN^{2-}) and $FMNH^-$. For the basic aqueous environment at pH 11, the pH is higher than the pK_a of FMN; thus, the species in solution before reduction is still the deprotonated fully oxidized flavin FMN^-, as confirmed by UV−vis spectroscopy. The reduced species present after bulk electrolysis is the same as in the other basic solutions, $FMNH^-$.

3.2. FMN (1 mM and 5 mM) and FAD (1 mM) in Unbuffered Aqueous Solutions. *3.2.1. Rationale Behind the Detailed Investigation of Flavins in Unbuffered Aqueous Solutions.* For unbuffered aqueous solutions, the proton concentration and thus the pH surrounding the electrode surface would be expected to change significantly during the cyclic voltammetry scans. Therefore, it was not expected that the same trends would be observed as for the buffered aqueous solutions.[23] It is possible that flavoenzymes in a biological environment that have the flavin moiety exposed to water might not always exist in a position that enables unhindered access of buffer molecules. For example, the bowl-shaped surface near the FMN-binding site in microsomal NADPH-

dx.doi.org/10.1021/jp4069619 | J. Phys. Chem. B 2013, 117, 13755−13766

cytochrome *c* reductase (where NADPH is the reduced form of nicotinamide adenine dinucleotide phosphate, $NADP^+$) has an opening approximately 6 Å in width, whereas the active site containing FAD in ferrodoxin-$NADP^+$-oxidoreductase and the active site in monomine oxidase A are more open.[35−39] Although it has been reported that the cytoplasm, mitochondrial cytosol, and endocytotic vesicles in cells are well buffered by proteins and the H_2CO_3/HCO_3^- system, the small 6-Å-wide crevice where the flavin moiety is located might not be buffered as well because both water and other molecules in the crevice are unable to flow freely and be replenished at the active sites. Therefore, the biological environment of some flavins could be similar to that of an unbuffered aqueous solution during cyclic voltammetry measurements, where the pH of the solution around the electrode surface changes rapidly even though that of the bulk solution remains unchanged. Furthermore, protein buffering, rather than H_2CO_3/HCO_3^- buffering, is considered to be dominant in cells.[40]

3.2.2. Cyclic Voltammetry of 1 mM FMN in Unbuffered Aqueous Solutions. Variable-scan-rate voltammetric experiments were performed in 1.0 mM FMN solutions at different pH values, from 2.13 to 11.03, as shown in Figure 5a, using small quantities of HCl or NaOH to vary the pH. Figures S5−S15 (Supporting Information) show the variable-scan-rate cyclic voltammograms of FMN in 0.2 M KCl, where current has been normalized by multiplying by $\nu^{-0.5}$ (where ν is the potential scan rate in V s^{-1}).

At low scan rates and low pH values (pH 2.13−3.08), only one distinctive redox wave appears at approximately $E^0 = -0.15$ V (wave 1), and the ratio of the oxidative (i_p^{ox}) and reductive (i_p^{red}) peak currents (i_p^{ox}/i_p^{red}) is equal to unity, indicating a chemically reversible reaction (Figure 5a). Wave 1 becomes broader when the pH increases from 2.13 to 3.08. It can also be observed that wave 1 shifts by −65 mV/ΔpH as the pH increases from pH 2.13 to pH 3.08, close to −59 mV/ΔpH, as expected for an nH^+/ne^- redox couple. Wave 1 is proposed to be a $2e^-/2H^+$ reduction, forming $(FMNH_2)H^-$, as sufficient protons are present for this reaction at low pH. (For the abbreviated names of the compounds, an H outside the parentheses indicates the protonation state of the phosphate groups, as shown in Scheme 4.) As the scan rate increases, the anodic (E_p^{ox}) and cathodic (E_p^{red}) peak-to-peak separation (ΔE_{pp}) of wave 1 does not substantially increase (beyond what is expected for solution resistance effects), which can be explained by fast heterogeneous electron-transfer and proton-transfer processes.

As the pH increases, the peak height of wave 1 drops, and another wave (wave 2) starts to appear at a more negative potential ($E^0 = -0.40$ V) and increases in size relative to wave 1. It is apparent that the decrease in the wave 1 reduction current corresponds to the increase in the amount of species responsible for wave 2. Wave 2 starts to appear at pH 3.57, at which the concentration of protons added is around 0.27 mM, significantly smaller than the 1.0 mM concentration of FMN in the solution. There are not enough protons for all of the flavins to undergo $2e^-/2H^+$ or $2e^-/H^+$ reduction, so it is postulated that the remainder of the fully oxidized flavins are reduced without any proton-transfer step. The peak potentials of wave 2 vary by only 50 mV over the intermediate pH values (from pH 3.98 to 7.11). Wave 2 was initially suspected to be a one-electron reduction process (because of its small peak currents) in which the fully oxidized flavin species $(FMN)H^-$ was reduced to form a flavosemiquinone radical species, $(FMN^{\bullet -})H^-$. However, it was observed that wave 2 is much broader and has a larger peak current than would be expected for a one-electron-transfer process, suggesting a two-electron

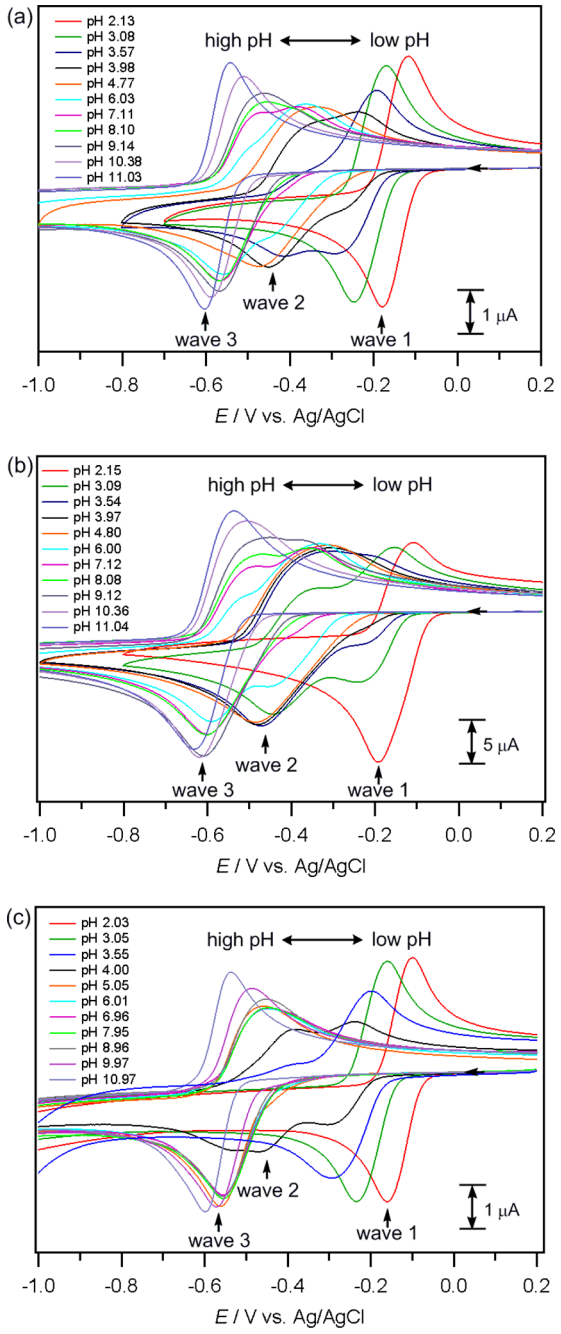

Figure 5. Cyclic voltammograms of (a) 1 mM FMN, (b) 5 mM FMN, and (c) 1 mM FAD in unbuffered aqueous solutions containing 0.4 M KCl at pH 2−11 using a 1-mm-diameter planar GC electrode at a scan rate of 0.1 V s^{-1}.

Scheme 4. Chemical Structures of Flavin Mononucleotide at Different Protonation States of the Phosphate Group

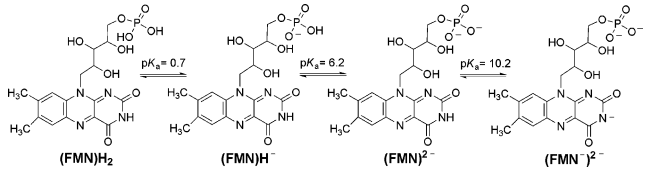

dx.doi.org/10.1021/jp4069619 | J. Phys. Chem. B 2013, 117, 13755−13766

reduction but with a much lower heterogeneous electron-transfer rate. Further experimentation with a rotating-disk electrode confirmed the two-electron transfer (see discussion in section 3.2.4).

The fact that the reduction potential of wave 2 changes by a relatively small amount at pH 4−7 suggests that wave 2 does not involve a protonation step from free acid and is thus independent of the pH change. Therefore, wave 2 is postulated to be a $2e^-$ reduction process through an EE mechanism (i.e., involving two closely spaced one-electron steps), forming $(FMN^{2-})H^-$, which undergoes further hydrogen bonding with H_2O. However, because of its basicity, $(FMN^{2-})H^-$ might be able to extract a proton from either a water molecule or another flavin molecule, as the flavins are in close proximity with one another asa result of the stacking of the isoalloxazine ring of FMN in aqueous solutions at concentrations above 50 μM.[41,42]

At pH 3.98, waves 1 and 2 both occur because of several species existing together in solution. A small number of the flavin radical anions, $(FMN^{\bullet-})H^-$, formed by the initial one-electron transfer undergo a protonation step forming $(FMNH^{\bullet})H^-$ prior to further reduction. The majority of the $(FMN^{\bullet-})H^-$ ions undergo a direct second reduction, forming the two-electron-reduced flavin species $(FMN^{2-})H^-$, which interacts with water through a hydrogen-bonding mechanism. At pH 4.77, the strongly pH-dependent wave 1 disappears entirely. One very broad and drawn-out process (wave 2) is observed, which is believed to be mainly associated with the $2e^-$ reduction of $(FMN)H^-$ to $(FMN^{2-})H^-$. The E^0 values of $(FMN)H^-/(FMN^{\bullet-})H^-$ and $(FMN^{\bullet-})H^-/(FMN^{2-})H^-$ are likely to be close enough for the peaks to merge into a single voltammetric wave, similar to the voltammetric behavior of quinones in organic solvents containing large amounts of water.[22] This is because $(FMN^{2-})H^-$ is strongly stabilized in water through hydrogen-bonding interactions, which facilitates the easier addition of an electron to the precursor $(FMN^{\bullet-})H^-$ species. Wave 2 is concluded to be associated with slower heterogeneous electron-transfer reactions, as it becomes broader and more spread out at higher scan rates. Wave 1 decreases in magnitude proportionally to wave 2 increasing in magnitude as the scan rate is increased. At higher scan rates, the protonation reaction of $(FMN^{\bullet-})H^-$ is outrun; hence, $(FMN^{\bullet-})H^-$ undergoes the second electron-transfer step, forming $(FMN^{2-})H^-$.

At pH 6.03, wave 2 decreases in size, and another chemically reversible wave (wave 3) begins to appear at approximately $E^0 = -0.52$ V. From pH 6.03 to 9.14, wave 2 decreases in peak height, with wave 3 concomitantly increasing in magnitude. The similarity between the peak height of wave 3 at high pH values (where only wave 3 is observed) and that of wave 1 at very low pH values (where only wave 1 is observed) suggests that wave 3 is also a two-electron reduction process. Further investigations using rotating-disk-electrode voltammetry confirmed the two-electron transfer.

3.2.3. Cyclic Voltammetry of 5 mM FMN in Unbuffered Aqueous Solutions. Variable-scan-rate voltammetric experiments were also conducted in solutions containing 5.0 mM FMN to probe the effects of the concentration of FMN on the voltammetric responses. The voltammetric response of 5.0 mM FMN showed a trend very similar to that of the 1 mM FMN solution, but with larger changes at every change in pH in the range of pH 2−4, as shown in Figure 5b.

In 5.0 mM FMN solution, the number of protons required in proton-coupled electron transfer (PCET) is 5 times higher than that in 1.0 mM FMN solution. Therefore, when the voltammograms of the 5.0 mM solution are compared with those of the 1.0 mM solution obtained at identical pH values, wave 1 is significantly smaller for the 5.0 mM FMN solution, whereas wave 2 is significantly larger. This means that wave 2 first appears at a lower pH of 3.09 (compared to pH 3.57 in 1.0 mM FMN solution), because the concentration of FMN (5 mM) already exceeds the concentration of free protons in the solution whereas, for the 1.0 mM FMN solution, there were still sufficient free protons at pH 3.09. The extreme sensitivity of wave 1 to the ratio of the concentrations of FMN and protons in solution further supports the hypothesis that wave 1 comprises a coupled $+2e^-/+2H^+$ reduction step. It was observed that increasing the concentration of FMN in solution mainly affected the voltammetric response of FMN at low pH values, where wave 1 was originally dominant. However, at pH 5 and higher, the voltammograms of 1.0 and 5.0 mM FMN at each pH are almost identical (Figure 5a,b). This also supports the hypothesis that waves 2 and 3 are proton-independent electron transfers.

3.2.4. Rotating-Disk-Electrode Voltammetry of 1 mM FMN in Unbuffered Aqueous Solutions. Unlike for FMN in buffered aqueous solutions, electrolysis experiments could not be performed in unbuffered aqueous solution at constant pH because of the large change in pH during the electrolysis process. After electrolysis of 1.0 mM FMN solution at pH 3.57, the final pH was found to be much higher, at 10.36, because of the protonation reaction that occurred. Rotating-disk-electrode (RDE) voltammetry was thus used instead to determine the number of electrons transferred in unbuffered solutions at different pH values.

RDE voltammetry was performed at a scan rate of 0.02 V s^{-1}, at which the noise level was minimal and current leveled off completely (Figure 6). In RDE voltammetry, the reduction of FMN was found to give very similar limiting current values at the three chosen pH values: 2.20 (only wave 1 observed), 4.80 (only wave 2 observed), and 9.13 (only wave 3 observed). As it was established that wave 1 is a proton-coupled $2e^-$ reduction, this finding provides substantial evidence that both waves 2 and 3 are also two-electron reduction processes.[23] At all pH values, the limiting current is proportional to the square root of the rotational velocity. It was observed that the slope of the graph at pH 4.80 was not as steep as that of pH 2.20 and pH 9.13, suggesting that wave 2, which contributes to the peak observed at pH 4.80, has a slower heterogeneous electron-transfer step(s). From these experiments, the diffusion coefficient of FMN was determined using Koutecký−Levich plots, by plotting the reciprocal of the limiting current against reciprocal of the square root of the rotational velocity, using the equations[43]

$$\frac{1}{I_c} = \frac{1}{0.62nF\pi r^2 D_A^{2/3} \nu^{-1/6} C_A^b} \frac{1}{\omega^{1/2}} + \frac{1}{nF\pi r^2 k_h C_A^b} \quad \text{(A)}$$

$$D_A = \left(\frac{1}{0.62nF\pi r^2 \nu^{-1/6} C_A^b} \frac{1}{\text{gradient}} \right)^{3/2} \quad \text{(B)}$$

where I_c is the limiting current (A), n is the number of electrons transferred (equiv mol^{-1}), F is the Faraday constant (96487 C $equiv^{-1}$), πr^2 is the geometric disk area (cm^2), D_A is the diffusion coefficient of the species of interest (cm^2 s^{-1}), ν is the kinematic viscosity (cm^2 s^{-1}), C_A^b is the bulk concentration of electroactive species (mol cm^{-3}), ω is the rotational velocity

dx.doi.org/10.1021/jp4069619 | J. Phys. Chem. B 2013, 117, 13755−13766

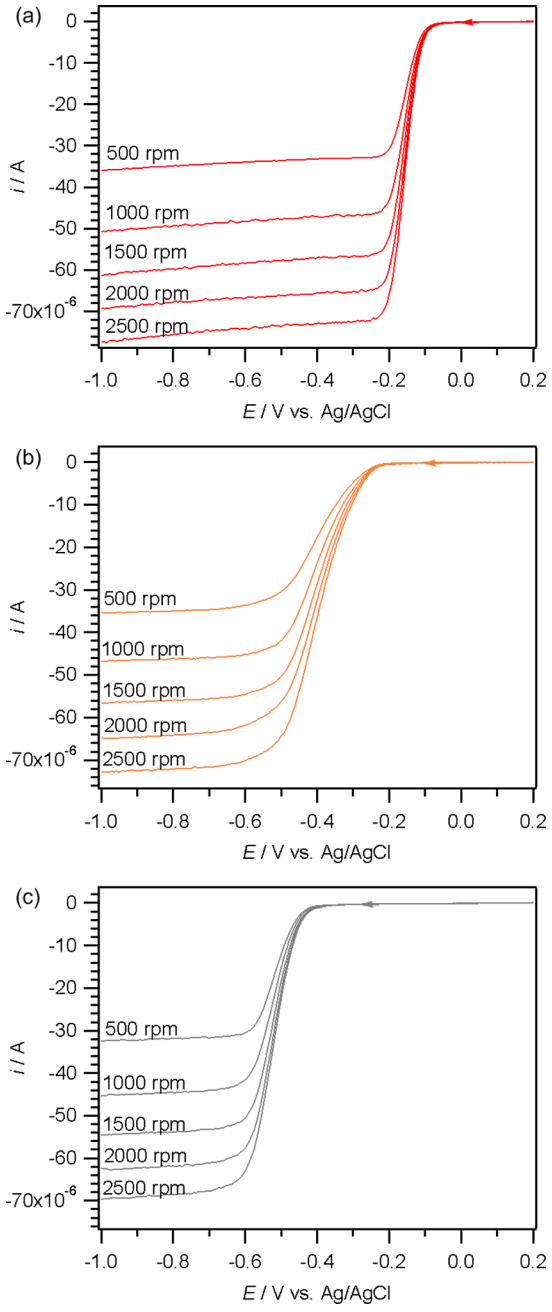

Figure 6. RDE voltammograms of 1.0 mM FMN in unbuffered 0.2 M KCl solution recorded using a 3-mm GC electrode at variable rotational velocities (500–2500 rpm) and a 0.02 V s^{-1} scan rate at pH (a) 2.20, (b) 4.80, and (c) 9.13.

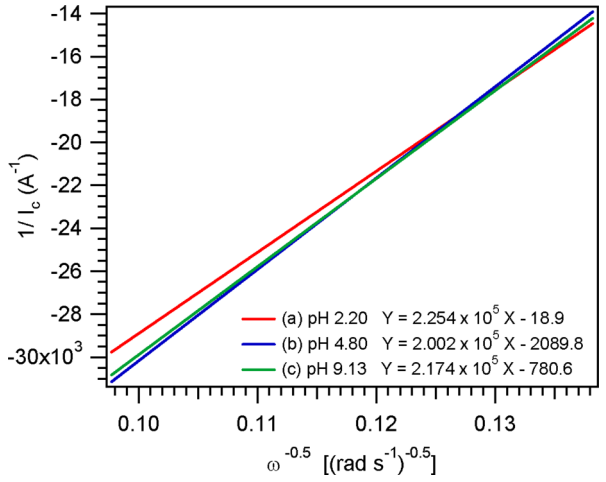

Figure 7. Koutecký–Levich plots of RDE voltammograms obtained at pH 2.20, 4.80, and 9.13.

(rad s^{-1}), and k_h is the heterogeneous rate constant of electron transfer (cm s^{-1}).

The plots at all three pH values show linear relationships between the reciprocal of the limiting current and the reciprocal of the square root of the rotational velocity (Figure 7). The gradient of the Koutecký–Levich plots can be used to calculate the diffusion coefficient of the species of interest using eq B.

Using the plot at pH 2.20, we determined the diffusion coefficient of FMN to be 3.80×10^{-6} cm^2 s^{-1}, which is close to the value obtained later by digital simulation of CV data.

3.2.5. Possible Involvement of the Phosphate Group in the Mechanism and Identification of Wave 3. It is hypothesized that wave 1 consists of a $2e^-/2H^+$ reduction of $(FMN)H^-$ to $(FMNH_2)H^-$ (proton-dependent) and that wave 2 consists of a $2e^-$ reduction of $(FMN)H^-$ to $(FMN^{2-})H^-$ (proton-independent), which occurs when there are insufficient protons present to form $(FMNH_2)H^-$. Moreover, it was confirmed by rotating-disk-electrode voltammetry that all three waves involve the transfer of the same number of electrons. However, the experiments described thus far did not allow for the identification of the reactions responsible for wave 3, other than it being a two-electron reduction process.

A 1.0 mM FMN solution (in 0.4 M KCl) has a pH of 5.7 before adjustment to more acidic or basic values. However, it was observed that significantly more NaOH had to be added to change the pH to more basic levels than the amount of HCl required to change the pH to more acidic levels. The exact amount of NaOH (in millimoles) required was recorded for each pH value, and it was observed that a 1.0 mM FMN solution required just under 1 equiv of NaOH to change the pH from 5.7 to 6.0. The final concentration of NaOH in solution was much higher than it should have been for pH 6.0, but it was the similarity of the concentrations of FMN and OH^- that led to the conclusion that OH^- was reacting with FMN in a 1:1 ratio to form a different flavin species. An initial hypothesis that OH^- was hydrogen-bonded to N(3)H was later discounted when the pK_a of the phosphate group on the flavin side chain was found to be 6.20.[29,44]

Therefore, a likely explanation for the fact that close to 1 equiv of NaOH had to be added to change the pH of the solution from 5.7 to 6.0 is that the OH^- added reacts with the protons that are released by the phosphate groups.

Thus, we postulate that, from pH 6.03 to 9.14, the phosphate fully deprotonated form, $(FMN)^{2-}$, undergoes reduction in wave 3 to form $(FMN^{\bullet -})^{2-}$ and $(FMN^{2-})^{2-}$. For the experiments performed in buffered solutions, the fully deprotonated form $[(FMN)^{2-}]$ is also present at sufficiently high pH, but the shift in voltammetric peak potentials over the pH range is controlled by the equilibrium expression in the Nernst equation involving the free acid, as well as protonation reactions of reduced flavins with the buffer electrolyte.

At pH 10.38 and 11.03, a slight shift in the reduction potential for wave 3 was observed. At these high pH values, the pH of the solution is near or higher than the pK_a of the N(3)H group on FMN; thus, FMN exists in the form of a mixture of $(FMN)^{2-}$ and the deprotonated form $(FMN^-)^{2-}$. The

dx.doi.org/10.1021/jp4069619 | J. Phys. Chem. B 2013, 117, 13755–13766

concentrations of $(FMN)^{2-}$ and $(FMN^{-})^{2-}$ at different pH values listed in Table 1 were computed using the Henderson–Hasselbalch equation

$$pH = pK_a + \log \frac{[(FMN^{-})^{2-}]}{[(FMN)^{2-}]} \quad (C)$$

Table 1. Concentrations of $(FMN)^{2-}$ and $(FMN^{-})^{2-}$ at Different pH Values, Calculated from $pK_a[(FMN)^{2-}] = 10.20$

pH	$[(FMN)^{2-}]$ (mM)	$[(FMN^{-})^{2-}]$ (mM)
9.14	0.920	0.080
10.38	0.398	0.602
11.03	0.148	0.852

The pK_a of FMN has been determined by several laboratories, and a few values have been reported. The reported values of the pK_a of FMN range between 9.65 and 10.40,[13,14,16,19,27−33] and the pK_a of FMN used in this study was 10.2, as recommended by Cerletti, obtained using absorption, fluorescence, and titration methods.[29] Because of its negative charge, the deprotonated flavin is harder to reduce than the protonated form, shifting the reduction potential to slightly more negative potentials. Thus, at pH 11, a mixture of hydrogen-bonded $(FMN^{3-})^{2-}$ and $(FMNH^{2-})^{2-}$ is formed.

Nevertheless, initially, we were skeptical that the minor change in the side chain would affect the electrochemical behavior of FMN, as it is far from the electroactive center. To understand this behavior better, we repeated the cyclic voltammograms at pH 2−11 using FAD, which also contains two phosphate groups (Scheme 1).

3.2.6. Cyclic Voltammetry of 1 mM FAD in Unbuffered Aqueous Solutions. When comparing the voltammograms of 1 mM FAD (Figure 5c) with those of 1 mM FMN (Figure 5a), the immediate difference observed is that wave 3 first occurs at pH 4 and above, instead of pH 6 and above (with FMN). Another difference is that wave 2 is prominent only at pH 4 for FAD and not at other pH values. As the pK_a values of the phosphate groups of FAD are 2.06 and 3.69,[45] at pH 4, FAD consists of a mixture of completely deprotonated and singly protonated phosphate groups. Thus, after protons are used up in wave 1, the remaining FAD molecules that are singly protonated undergo reduction in wave 2, and those that are completely deprotonated undergo reduction in wave 3. The presence of wave 3 occurring after both phosphate groups are deprotonated is in good agreement with our results from FMN, where wave 3 occurs only when the phosphate group is completely deprotonated (pH 6 and higher), giving further evidence that the charge on the phosphate group affects the electrochemistry of the flavins.

The effect that the negative charge on the phosphate group has on the electrochemistry of the flavins could result from electrostatic interactions with a positive dipole at the electroactive center of the flavin, forming a partial negative charge at the electroactive center and thus making it harder to reduce (wave 3 occurs at more negative potentials than wave 2).

3.2.7. Electron-Transfer Mechanism of FMN in Unbuffered Aqueous Solutions. The complete electrochemical reduction mechanisms of FMN in unbuffered aqueous solution are given in Schemes 5−7, based on the CV experiments conducted with

Scheme 5. Voltammetrically Induced Proton-Coupled Electron-Transfer Reduction Mechanism of FMN in Unbuffered Aqueous Solutions at pH 2.13−6.03 over a Range of Scan Rates

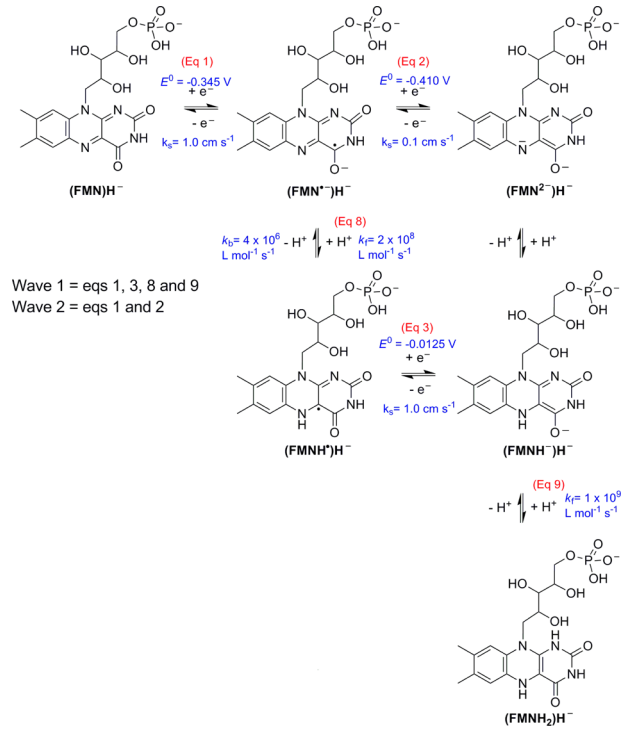

Scheme 6. Voltammetrically Induced Electron-Transfer Reduction Mechanism of FMN in Unbuffered Aqueous Solutions at pH 6.03−9.14 over a Range of Scan Rates

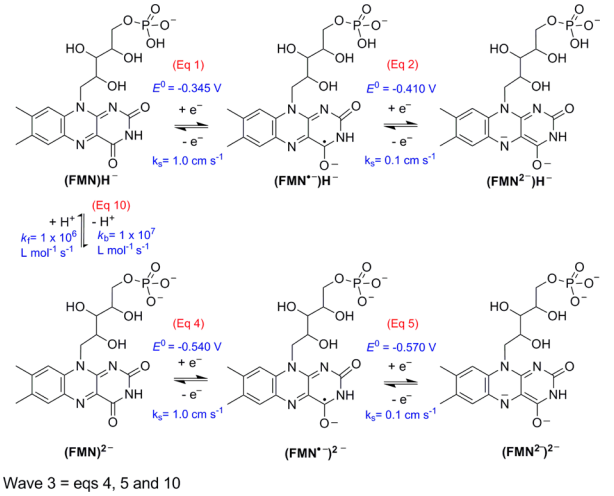

1.0 mM FMN in 0.4 M of KCl solution. The mechanisms in Schemes 5−7 were refined by performing digital fitting of the electrochemical data obtained at the different pH values using the commercially available DigiElch software package, until the variable simulation parameters (electrode potentials, rate constants, and equilibrium constants) provided simulated voltammograms that closely matched the experimental curves (Figure 8). The final optimized parameters used in the digital simulations for the mechanisms in Schemes 5−7 are reported in Tables 2 and 3. The concentrations of H^+ and OH^- used in the simulations were set according to the amount of acid or

dx.doi.org/10.1021/jp4069619 | J. Phys. Chem. B 2013, 117, 13755−13766

Scheme 7. Voltammetrically Induced Electron-Transfer Reduction Mechanism of FMN in Unbuffered Aqueous Solutions at pH 10.38−11.03 over a Range of Scan Rates

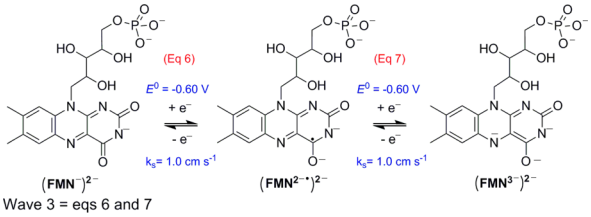

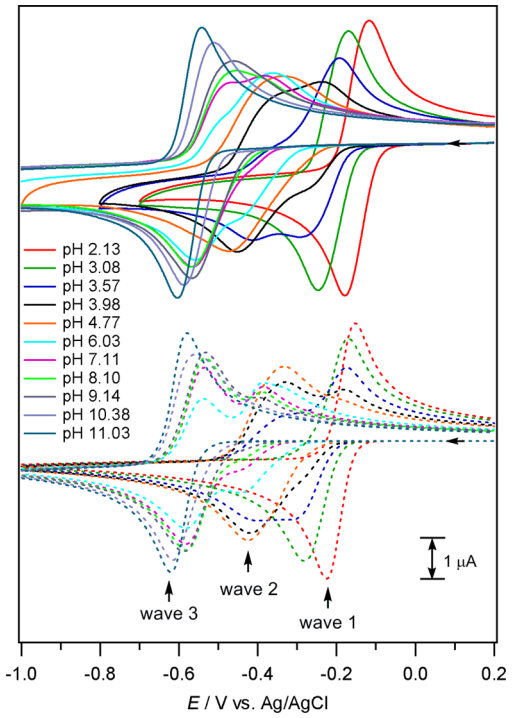

Figure 8. Cyclic voltammograms of 1.0 mM FMN in 0.4 M KCl recorded at a 1-mm GC electrode (solid lines) and digital simulations of the CV data based on the mechanism in Schemes 5−7 and parameters given in Tables 1 and 2 (dotted lines).

base added during the experiment to reflect the change in pH. To adjust to acidic pH values (pH 2.13−4.77), hydrochloric acid was added, whereas to alter to alkaline pH values (pH 6.03−11.03), sodium hydroxide was added.

Good matches between the experimental and simulated results were obtained by using parameters listed in Tables 2 and 3, with the simulated voltammograms shown in Figures 8 and S37 (Supporting Information). The peak heights of the simulated graphs fit very closely with those of the experimental graphs. A shift in peak potential and decrease in peak height are observed in wave 1 from pH 2.13 to 4.77. $(FMN)H^-$ is first reduced by one electron to form $(FMN^{\bullet-})H^-$ at a potential of $E^0 = -0.345$ V and then receives a proton to form $(FMNH^{\bullet})H^-$. The protonated radical $[(FMNH^{\bullet})H^-]$ is then reduced at a less negative potential ($E^0 = -0.0125$ V), forming $(FMNH^-)H^-$. This anionic species and its protonated form, $(FMNH_2)H^-$, depend on the amount of protons available in the solution. The reactions in eqs 1, 8, 3, and 9 (Scheme 5) give rise to wave 1. Wave 2 appears at pH 3.57 and starts increasing in size as the pH increases. When there are minimal protons in the solution, $(FMN^{\bullet-})H^-$ is further reduced to $(FMN^{2-})H^-$ shown by eqs 1 and 2 in Schemes 5 and 6. Wave 3 occurs at high pH values, where we postulate that $(FMN)^{2-}$ (with the phosphate group fully deprotonated) undergoes $2e^-$ reduction as in eqs 4 and 5 in Scheme 6 and where $(FMN^-)^{2-}$ (with the phosphate group fully deprotonated) undergoes $2e^-$ reduction as in eqs 6 and 7 in Scheme 7.

3.3. Relevance of Electrochemical Results to Flavoproteins and Further Applications. Based on the current results and past research, it is important to note that the redox properties and mechanisms of flavins are highly sensitive to the physical environment in which the flavin is located, which is one of the unique advantages of flavin as a coenzyme. Not only are the behaviors of free flavins different depending on whether the flavins are in an aprotic hydrophobic environment, a buffered aqueous environment, or an unbuffered aqueous environment, but also the behavior of flavins in each flavoenzyme also differs depending on the intermolecular interactions between flavin and the enzyme. An interesting example is assimilatory nitrate reductase from *Chlorella vulgaris*: The fully reduced flavin form was $FADH^-$, whereas the NADH-reduced sample showed the formation of $FAD^{\bullet-}$ instead.[46] Also, binding of NAD^+ to cytochrome b_5 reductase causes changes in intermolecular interactions between the enzyme and $FADH_2$, which stabilizes the semiquinone form and allows the donation of one electron to one-electron acceptors.[8] The rates of electron shuttling between OM c-Cyt complexes and the electrode surface for the two-electron redox process of free flavins are increased when the flavin is bound in OM c-Cyt, which promotes a one-electron redox process forming a semiquinone.[47]

It would appear to be simpler to analyze each flavoenzyme separately; however, the low heterogeneous electron-transfer rates for flavoenzymes continue to cause difficulties in finding the detailed electron-transfer mechanism of each flavoenzyme. Thus, it is useful to form deductions based on the closest model. For flavoenzymes with flavins in aqueous environments, care must be exercised before assuming that the active site of

Table 2. Electrochemical Parameters[a] Obtained by Digital Simulation of CV Data[b] for the Reaction Mechanism Given in Schemes 5−7

	eq 1: $(FMN)H^- + e^- \rightleftharpoons (FMN^{\bullet-})H^-$		eq 2: $(FMN^{\bullet-})H^- + e^- \rightleftharpoons (FMN^{2-})H^-$		eq 3: $(FMNH^{\bullet})H^- + e^- \rightleftharpoons (FMNH^-)H^-$		eq 4: $(FMN)^{2-} + e^- \rightleftharpoons (FMN^{-\bullet})^{2-}$		eq 5: $(FMN^{-\bullet})^{2-} + e^- \rightleftharpoons (FMN^{2-})^{2-}$		eq 6: $(FMN^-)^{2-} + e^- \rightleftharpoons (FMN^{2-\bullet})^{2-}$		eq 7: $(FMN^{2-\bullet})^{2-} + e^- \rightleftharpoons (FMN^{3-\bullet})^{2-}$	
D ($cm^2\ s^{-1}$)	$E^0_{(1)}$ (V)	$k_{s(1)}$ ($cm\ s^{-1}$)	$E^0_{(2)}$ (V)	$k_{s(2)}$ ($cm\ s^{-1}$)	$E^0_{(3)}$ (V)	$k_{s(3)}$ ($cm\ s^{-1}$)	$E^0_{(4)}$ (V)	$k_{s(4)}$ ($cm\ s^{-1}$)	$E^0_{(5)}$ (V)	$k_{s(5)}$ ($cm\ s^{-1}$)	$E^0_{(6)}$ (V)	$k_{s(6)}$ ($cm\ s^{-1}$)	$E^0_{(7)}$ (V)	$k_{s(7)}$ ($cm\ s^{-1}$)
3.0×10^{-6}	−0.345	1	−0.41	0.1	−0.0125	1	−0.54	1	−0.57	1	−0.60	1	−0.60	1

[a] D = diffusion coefficient, E^0 = formal reduction potential, k_s = heterogeneous electron-transfer rate constant. [b] CV data recorded in unbuffered aqueous solutions at 22 (±2) °C with 0.4 M KCl as the supporting electrolyte with a 1-mm-diameter planar GC working electrode at a scan rate of 0.1 V s^{-1}.

dx.doi.org/10.1021/jp4069619 | J. Phys. Chem. B 2013, 117, 13755−13766

Table 3. Equilibrium (K_{eq}) Constants and Forward (k_f) and Backward (k_b) Rate Constants Obtained by Digital Simulation of CV Data for the Reaction Mechanism Given in Schemes 5−7 Obtained in Unbuffered Aqueous Solution Containing 0.4 M KCl at 22 (±2) °C

eq 8: $(FMN^{\bullet -})H^- + H^+ \rightleftharpoons (FMNH^{\bullet})H^-$			eq 9: $(FMNH^-)H^- + H^+ \rightleftharpoons (FMNH_2)H^-$			eq 10: $(FMN)H^- \rightleftharpoons (FMN)^{2-} + H^+$			eq 11: $H_2O \rightleftharpoons H^+ + OH^-$
$K_{eq(1)}$	$k_{f(1)}$ (L mol^{-1} s^{-1})	$k_{b(1)}$ (s^{-1})	$K_{eq(2)}$	$k_{f(2)}$ (L mol^{-1} s^{-1})	$k_{b(2)}$ (s^{-1})	$K_{eq(3)}$	$k_{f(3)}$ (L mol^{-1} s^{-1})	$k_{b(3)}$ (s^{-1})	$K_{eq(4)}$
50	2.00×10^8	4.00×10^6	50	1.00×10^9	2.00×10^7	1.00×10^{-7}	500	5.00×10^9	1.00×10^{-14}

the flavoprotein is as well buffered as the cell cytoplasm in which the flavoprotein is located, considering the differences in the electrochemical reactions between flavins in aqueous buffered solution and those in aqueous unbuffered solution.

To decipher which mechanism is most applicable to each flavoenzyme, it is important to analyze the crystal structure of the flavoenzyme, to determine whether the flavin cofactor is buried in a completely hydrophobic environment, freely accessible to solvent molecules, or buried in a bowl-shaped surface with a small entry point for solvent molecules. It might also be important to note whether the side chain of the flavin is buried within the flavoenzyme or readily accessible to the isoalloxazine ring and whether free flavin is present in the flavoenzyme, as a doubly charged phosphate group could affect the electron-transfer mechanism. It is also worth noting that, in aqueous unbuffered solutions, FMN and FAD behave slightly differently in the range of pH 3−7.

4. CONCLUSIONS

Bulk controlled potential electrolysis experiments have confirmed that the net electrochemical reduction of FMN in buffered aqueous solutions at pH 3−11 occurs by two electrons per molecule. UV−vis spectroscopic experiments conducted after bulk electrolysis showed that the major reduced species present in the bulk solution for pH 3−5 is different from that at pH 7−10, consisting of $FMNH_2$ and $FMNH^-$, respectively. CV experiments conducted at high pH and low scan rates showed a significantly broadened oxidation peak that separated into two oxidation peaks when the scan rate was increased. However, with increasing scan rate, the second oxidation peak also decreased in size, indicating that the protonation reaction of the hydrogen-bonded dianion to form $FMNH^-$ was outrun.

Significantly different results were observed for FMN in unbuffered aqueous solutions, showing that differences in the buffer capacity in the active sites of flavoenzymes could lead to the occurrence of different mechanisms. Three different waves were observed for three pH ranges: wave 1 at very low pH, where the concentration of protons is equal to or higher than that of FMN; wave 2 at midrange pH values, generally pH 3.5−6; and wave 3 at higher pH, where the pH is higher than the pK_{a2} of the phosphate group. Rotating-disk-electrode voltammetry confirmed that all three waves consist of a two-electron reduction mechanism. Comparisons of the cyclic voltammograms of 1 and 5 mM FMN confirmed that wave 1 was a proton-dependent electron transfer whereas waves 2 and 3 were proton-independent. Comparisons of the cyclic voltammograms of 1 mM FMN and 1 mM FAD indicated that wave 3 occurs only when the phosphate groups are completely deprotonated. This provides evidence that the charge on the phosphate groups affects the electron-transfer mechanism of FMN.

■ ASSOCIATED CONTENT

Supporting Information

Variable-scan-rate cyclic voltammograms of 1 mM FMN in buffered aqueous solutions obtained at different pH values (pH 3−11), variable-scan-rate cyclic voltammograms of 1 and 5 mM FMN and 1 mM FAD in unbuffered aqueous solutions obtained at different pH values (pH 2−11) at a 1-mm-diameter GC electrode, and digitally simulated cyclic voltammograms of 5 mM FMN. This material is available free of charge via the Internet at http://pubs.acs.org.

■ AUTHOR INFORMATION

Corresponding Author

*E-mail: webster@ntu.edu.sg. Tel.: +65 6316 8793.

Notes

The authors declare no competing financial interest.

■ ACKNOWLEDGMENTS

This work was supported by an A*Star SERC Public Sector Funding (PSF) Grant (112 120 2006). S.L.J.T. thanks NTU for the award of a Nanyang President's Graduate Scholarship (NPGS).

■ REFERENCES

(1) Walsh, C. Flavin Coenzymes: At the Crossroads of Biological Redox Chemistry. *Acc. Chem. Res.* **1980**, *13*, 148−155.
(2) Ghisla, S.; Massey, V. Mechanisms of Flavoprotein-Catalyzed Reactions. *Eur. J. Biochem.* **1989**, *181*, 1−17.
(3) Bruice, T. C. Oxygen−Flavin Chemistry. *Isr. J. Chem.* **1984**, *24*, 54−61.
(4) Mueller, F. In *Topics in Current Chemistry*; Boschke, F. L., Ed.; Springer-Verlag: Berlin, 1983; Vol. *108*, pp 71−108.
(5) Niemz, A.; Imbriglio, J.; Rotello, V. M. Model Systems for Flavoenzyme Activity: One- and Two-Electron Reduction of Flavins in Aprotic Hydrophobic Environments. *J. Am. Chem. Soc.* **1997**, *119*, 887−892.
(6) Massey, V.; Hemmerich, P. Active-Site Probes of Flavoproteins. *Biochem. Soc. Trans.* **1980**, *8*, 246−257.
(7) Paulsen, K. E.; Stankovich, M. T.; Stockman, B. J.; Markley, J. L. Redox and Spectral Properties of Flavodoxin from Anabaena 7120. *Arch. Biochem. Biophys.* **1990**, *280*, 68−73.
(8) Iyanagi, T. Redox Proprties of Microsomal Reduced Nicotinamide Adenine Dinucleotide-Cytochrome b_5 Reductase and Cytochrome b_5. *Biochemistry* **1977**, *16*, 2725−2730.
(9) Iyanagi, T.; Watanabe, S.; Anan, K. F. One-Electron Oxidation−Reduction Properties of Hepatic NADH−Cytochrome b_5 Reductase. *Biochemistry* **1984**, *23*, 1418−1425.
(10) Nishida, H.; Inaka, K.; Yamanaka, M.; Kaida, S.; Kobayashi, K.; Miki, K. Crystal Structure of NADH−Cytochrome b_5 Reductase from Pig Liver at 2.4 Å Resolution. *Biochemistry* **1995**, *34*, 2763−2767.
(11) Tan, S. L. J.; Webster, R. D. Electrochemically Induced Chemically Reversible Proton-Couple Electron Transfer Mechanisms of Riboflavin (Vitamin B_2). *J. Am. Chem. Soc.* **2012**, *134*, 5954−5964.
(12) Janik, B.; Elving, P. J. Polarographic Behavior of Nucleosides and Nucleotides of Purines, Pyrimidines, Pyridines and Flavins. *Chem. Rev.* **1968**, *68*, 295−319.

(13) Michaelis, L.; Schwarzenbach, G. The Intermediate Forms of Oxidation−Reduction of the Flavins. *J. Biol. Chem.* **1938**, *123*, 527−542.
(14) Draper, R. D.; Ingraham, L. L. A Potentiometric Study of the Flavin Semiquinone Equilibrium. *Arch. Biochem. Biophys.* **1968**, *125*, 802−808.
(15) Hartley, A. M.; Wilson, G. S. Unusual Adsorption Effects in the Electrochemical Reduction of Flavin Mononucleotide at Mercury Electrodes. *Anal. Chem.* **1966**, *38*, 681−687.
(16) Lowe, H. J.; Clark, W. M. Studies on Oxidation−Reduction: Oxidation−Reduction Potentials of Flavin Adenine Dinucleotide. *J. Biol. Chem.* **1956**, *220*, 983−992.
(17) Wei, H.; Omanovic, S. Interaction of Flavin Adenine Dinucleotide (FAD) with a Glassy Carbon Electrode Surface. *Chem. Biodiv* **2008**, *5*, 1622−1639.
(18) Cable, M.; Smith, E. T. Identifying the n = 2 Reaction Mechanism of FAD through Voltammetric Simulations. *Anal. Chim. Acta* **2005**, *537*, 299−306.
(19) Ksenzhek, O. S.; Petrova, S. A. Electrochemical Properties of Flavins in Aqueous Solutions. *Bioelectrochem. Bioenerg.* **1983**, *11*, 105−127.
(20) Diculescu, V. C.; Militaru, A.; Shah, A.; Qureshi, R.; Tugulea, L.; Brett, A. M. O. Redox Mechanism of Lumazine at a Glassy Carbon Electrode. *J. Electroanal. Chem.* **2010**, *647*, 1−7.
(21) Male, R.; Samotowka, M. A.; Allendoerfer, R. D. Simultaneous Electrochemical and EPR Studies of Flavin Radical Equilibria. *Electroanalysis* **1989**, *1*, 333−339.
(22) Hui, Y.; Chng, E. L. K.; Chng, C. Y. L.; Poh, H. L.; Webster, R. D. Hydrogen-Bonding Interactions between Water and the One- and Two-Electron-Reduced Forms of Vitamin K1: Applying Quinone Electrochemistry to Determine the Moisture Content of Non-Aqueous Solvents. *J. Am. Chem. Soc.* **2009**, *131*, 1523−1534.
(23) Quan, M.; Sanchez, D.; Wasylkiw, M. F.; Smith, D. K. Voltammetry of Quinones in Unbuffered Aqueous Solution: Reassessing the Roles of Proton Transfer and Hydrogen Bonding in Aqueous Electrochemistry of Quinones. *J. Am. Chem. Soc.* **2007**, *129*, 12847−12856.
(24) Nöll, G. Spectroscopic Investigation of Flavoproteins: Mechanistic Differences between (Electro)chemical and Photochemical Reduction and Oxidation. *J. Photochem. Photobiol. A* **2008**, *200*, 34−38.
(25) Hemmerich, P.; Veeger, C.; Wood, H. C. S. Fortschritte in Chemie und Molekularbiologie der Flavin und Flavocoenzyme. *Angew. Chem.* **1965**, *77*, 699−716.
(26) Dudley, K. H.; Ehrenberg, A.; Hemmerich, P.; Müller, F. Spektren und Strukturen der am Flavin-Redoxsystem beteiligten Partikeln. *Helv. Chim. Acta* **1964**, *47*, 1354−1383.
(27) Mayhew, S. G. The Effects of pH and Semiquinone Formation on the Oxidation−Reduction Potentials of Flavin mononucleotide. *Eur. J. Biochem.* **1999**, *265*, 698−702.
(28) Ke, B. Polarography of Flavine Mononucleotide and Flavine Adenine Dinucleotide. *Arch. Biochem. Biophys.* **1957**, *68*, 330−340.
(29) Cerletti, P. Properties of Riboflavin Phosphates. *Anal. Chim. Acta* **1959**, *20*, 243−250.
(30) Michaelis, L.; Schubert, M. P.; Smythe, C. V. Potentiometric Study of the Flavins. *J. Biol. Chem.* **1936**, *116*, 587−607.
(31) Albert, A. Quantitative Studies of the Avidity of Naturally Occurring Substances for Trace Metals: Pteridines, Riboflavin and Purines. *Biochem. J.* **1953**, *54*, 646−654.
(32) Heelis, P. F. The Photophysical and Photochemical Properties of Flavins (Isoalloxazines). *Chem. Soc. Rev.* **1982**, *11*, 15−39.
(33) Stare, F. J. A Potentiometric Study of Hepatoflavin. *J. Biol. Chem.* **1935**, *112*, 223−229.
(34) Malinowski, E. R.; Barber, M. J.; Whitaker, G. T.; Smith, E. T. Factor Analysis of the Spectroelectrochemical Reduction of FAD Reveals the pK_a of the Reduced State and the Reduction Pathway. *J. Chemom.* **2007**, *21*, 520−528.
(35) Bruns, C. M.; Karplus, P. A. Refined Crystal Structure of Spinach Ferrodoxin Reductase at 1.7 Å Resolution: Oxidized, Reduced and 2′-Phospho-5′-AMP Bound States. *J. Mol. Biol.* **1995**, *247*, 125−145.
(36) Mattevi, A. To Be or Not To Be an Oxidase: Challenging the Oxygen Reactivity of Flavoenzymes. *Trends Biochem. Sci.* **2006**, *31*, 276−283.
(37) Edmondson, D. E.; Binda, C.; Mattevi, A. The FAD Binding Sites of Human Monoamine Oxidases A and B. *Neurotoxicology* **2004**, *25*, 63−72.
(38) Edmondson, D. E.; Binda, C.; Mattevi, A. The FAD Binding Sites of Human Monoamine Oxidases A and B. *Neurotoxicology* **2004**, *25*, 63−72.
(39) Edmondson, D. E.; Binda, C.; Wang, J.; Upadhyay, A. K.; Mattevi, A. Molecular and Mechanistic Properties of the Membrane-Bound Mitochondrial Monoamine Oxidases. *Biochemistry* **2009**, *48*, 4220−4230.
(40) Durand, T.; Vidal, G.; Canioni, P.; Gallis, J.-L. Cytosolic pH Variations in Perfused Rat Liver at 4°C: Role of Intracellular Buffering Power. *Cryobiology* **1998**, *36*, 269−278.
(41) Müller, F.; Mayhew, S. G.; Massey, V. On the Effect of Temperature on the Absorption Spectra of Free and Protein-Bound Flavines. *Biochemistry* **1973**, *12*, 4654−4662.
(42) Sarma, R. H.; Dannies, P.; Kaplan, N. O. Investigations of Inter- and Intramolecular Interactions in Flavin−Adenine Dinucleotide by Proton Magnetic Resonance. *Biochemistry* **1968**, *7*, 4359−4367.
(43) Treimer, S.; Tang, A.; Johnson, D. C. A Consideration of the Application of Koutecký−Levich Plots in the Diagnoses of Charge-Transfer Mechanisms at Rotated Disk Electrodes. *Electroanalysis* **2002**, *14*, 165−171.
(44) Tsentalovich, Y. P.; Lopez, J. J.; Sagdeev, R. Z. Mechanisms of Reactions of Flavin Mononucleotide Triplet with Aromatic Amino Acids. *Spectrochim. Acta* **2002**, *58*, 2043−2050.
(45) Bidwell, J.; Thomas, J.; Stuehr, J. Thermodynamic and Kinetic Study of the Interactions of Ni(II) with FMN and FAD. *J. Am. Chem. Soc.* **1986**, *108*, 820−825.
(46) Kay, C. J.; Solomonson, L. P.; Barber, M. J. Oxidation−Reduction Potentials of Flavin and Mo−Pterin Centers in Assimilatory Nitrate Reductase: Variation with pH. *Biochemistry* **1990**, *29*, 10823−10828.
(47) Okamoto, A.; Hashimoto, K.; Nealson, K. H.; Nakamura, R. Rate Enhancement of Bacterial Extracellular Electron Transport Involves Bound Flavin Semiquinones. *Proc. Natl. Acad. Sci. U.S.A.* **2013**, *110*, 7856−7861.